09

The effect of the pump pulse duration and duty cycle on power characteristics of quantum cascade lasers

© V.V. Dudelev[1], E.D. Cherotchenko[1], I.I. Vrubel[1], D.A. Mikhailov[1], D.V. Chistyakov[1], S.N. Losev[1], A.V. Babichev[1], E.A. Kognovitskaya[1], A.V. Lyutetskii[1], S.O. Slipchenko[1], N.A. Pikhtin[1], A.G. Gladyshev[2], I.I. Novikov[2,3], V.I. Kuchinskii[1], D.S. Papylev[3], L.Ya. Karachinsky[2,3], A.Yu. Egorov[2], G.S. Sokolovskii[1]

[1] Ioffe Institute, St. Petersburg, Russia
[2] „Connector Optics" LLC, St. Petersburg, Russia
[3] ITMO University, St. Petersburg, Russia
E-mail: v.dudelev@mail.ru

Received November 1, 2024
Revised November 13, 2024
Accepted November 13, 2024

We experimentally and theoretically investigated the quantum cascade lasers (QCLs) characteristics at various duty cycles and different repetition rates of pumping pulses. We show theoretically and experimentally that short-pulse pumping should be used to obtain high average power while maintaining peak power values. The maximum average output power of more than 100 mW has been experimentally demonstrated. Further increase in average power requires better heat dissipation from the active region.

Keywords: integrated optics, quantum cascade laser.

DOI: 10.61011/TPL.2025.02.60646.20177

Quantum-cascade lasers (QCLs) is a rapidly growing class of coherent emitters for the mid-infrared range. Their high output power and efficiency largely depend on the temperature stability of the output characteristics, primarily on the temperature stability of the threshold current. This is mainly due to the fact that high operating voltages and low thermal conductivity of the active region materials lead to its strong heating even at pumping with short current pulses [1].

A separate area of research is using QCLs to generate and transmit data. This includes studies of random number generation based on cascade lasers [2,3] as well as the development of mid-infrared wireless optical communication systems [4]. These and many other applications require temperature stability of QCLs when operating in continuous or pulsed mode with high filling factor. Therefore, the efforts of researchers are focused on developing new active region designs that provide high temperature stability of QCLs. In [5], a characteristic temperature of $T_0 \sim 380$ K was demonstrated for the $4-5\,\mu$m, spectral range of QCLs, which allowed this design to achieve efficiencies of over 30% in pulsed mode [6] and over 20% in continuous mode generation [7]. Also for longer wavelength QCLs T_0 over 170 K at efficiencies of $\sim 20\%$ [8] and even over 240 K at efficiencies over 10% [9] were shown. In all cases, the approach to improving the threshold properties of QCLs is the development of active region designs based on voltage-balanced pit/barrier layers, which provide a large energy gap at the hetero-boundary, allowing to reduce the thermal release of charge carriers from the upper laser level into the continuum.

In this paper, the pulsed modes of QCL operation at different filling factors have been investigated. In the experiment we used QCLs of the $8\,\mu$m spectral range with an active region based on InGaAs/InAlAs well/barrier pair with fifty quantum stages lattice matched to InP substate. A detailed description of the structure is given in [10].

QCL stripes were formed by etching two deep grooves $\sim 9\,\mu$m deep. The width of the formed stripe along the top edge was $\sim 10\,\mu$m. Details of the post-growth procedure are outlined in [11]. After the post-growth processing, the wafer was divided into 3 mm long chips, which were mounted epitaxial layer down for better heat dissipation from the active region.

Fig. 1 shows the dependencies of the maximum peak power and maximum average power on the filling factor. The QCL studies were carried out in pulsed mode at different values of the filling factor at a pulse repetition rate of 10 kHz. The QCL radiation was collimated by a germanium alloy aspherical lens with an effective focal distance of 0.7 mm and a numerical aperture of 0.85. The working surfaces of the lens were coated with a broadband antireflection coating that provided a Fresnel reflection loss of less than 1%. The collimated beam was split in a 1/9 ratio using an BaF_2wafer. The smaller portion of the radiation was directed to a fast-acting CdHgTe photodetector (CdHgTe — cadmium−mercury −tellurium) with four-stage cooling. This photodetector, connected to an oscilloscope, allowed the precise shape of the optical pulse to be recorded. The average P_{av} power was recorded using a Thorlabs PM100D verified power meter with an S401C thermoelectric detector. In the average power readings, 10% of the power was detached to the CMT photodetector. The

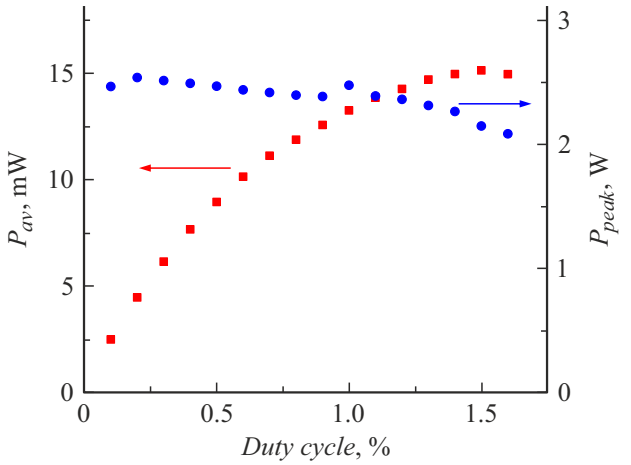

Figure 1. Dependence of peak power (circles) and average power (squares) on the filling factor. Hereinafter, the power from two QCL mirrors is given.

peak power P_{peak} was calculated using a simple expression

$$P_{peak} = \frac{A_m P_{av}}{Sf}, \qquad (1)$$

where A_m — the maximum amplitude of the optical pulse, S — the oscillogram area of the optical pulse [V·s], f — the pulse repetition rate [Hz]. Although the maximum value of the filling factor is small and is not more than 1.6%, the results clearly indicate that the QCL overheats once the filling factor increases beyond 0.3%. It is after this value that a decrease in peak power is observed, as well as a deviation from the linear relationship of the average power value. The results obtained show that it is necessary to properly select the pulse pumping modes to reduce the influence of overheating of the active region of the QCL in order to achieve an optimal balance between the pulse and average power of the output radiation.

To analyze the influence of the pumping mode of the laser on its parameters, we used the numerical solution of the nonequilibrium heat conduction equation squared 0.2×0.2 mm with the thermal engineering parameters of the laser design elements given in [1]. We have considered two limiting cases of heat dissipation efficiency. In the first case in the model, the massive copper heat sink had full contact with the laser chip, while in the other case it was effectively isolated. The width of the structure was chosen to be $20\,\mu$m, which corresponded to the width of the base of the samples strip studied. We considered the pump pulse durations of 100 and 1000 ns. The dynamics of the core center temperature change over the $100\,\mu$s interval in double logarithmic scale for four combinations of heat sink and pulse duration is shown in Fig. 2. It can be seen that when a current pulse of 2 A and 100 and 1000 ns duration is applied, the laser core center overheats by 7 and 20 K, respectively. Then, after the pump pulse is turned off, the temperature decreases according to a

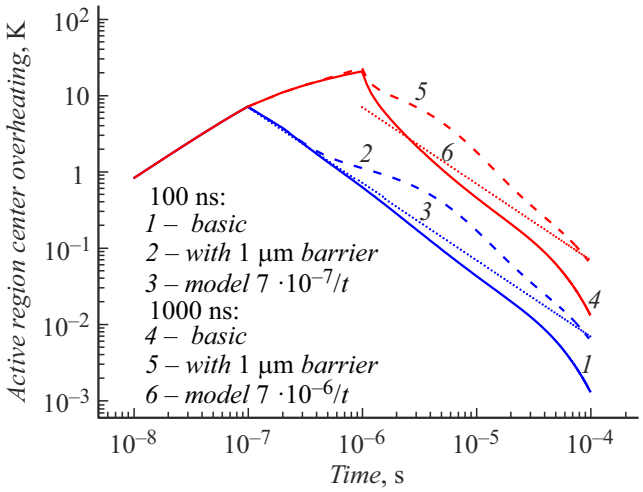

Figure 2. Temporal dynamics of the temperature of the QCL core center calculated by solving the two-dimensional unsteady heat conduction equation and plotted on a double logarithmic scale. The lines *1–3* show the evolution of the core center temperature when pumped by a 100 ns pulse, the lines *4–6* — 1000 ns. The solid lines *1, 4* — the results of the model with a working copper heat sink, the dashed lines *2, 5* — with an isolated heat sink, the dotted lines *3, 6* — approximating functions of the form t^{-1} (t — time). The amplitude of the pump current is $I = 2$ A. For the parameters of this calculation, the values of equilibrium superheat in the linear response approximation are $T_{eq}(1000\,\text{ns}) = 1.1$ K, $T_{eq}(100\,\text{ns}) = 1.3$ K, while the average pulse superheat for these cases is $\langle T_{imp}\rangle(1000\,\text{ns}) = 14$ K and $\langle T_{imp}\rangle(100\,\text{ns}) = 3$ K respectively.

complex law obeying the nonequilibrium heat conduction equation without internal heat sources. The small size and the filling factor allow the core to be considered as an instantaneous point source of heat for the entire QCL structure. In the case of two-dimensional geometry of the structure, the temporal and spatial evolution of the released energy, or the Green's function of the instantaneous heat source, has the following form:

$$T(\rho, t) = \frac{\Theta(t)}{4\pi k t} e^{-\frac{\rho^2}{4kt}}, \qquad (2)$$

where ρ — distance from the instantaneous heat release point, k — diffusion coefficient, [cm^2/s], $\Theta(t)$ — Heaviside function. Since the cross-sectional area of the QCL is much smaller than that of the heat sink, after the pump is turned off in the $\rho \to 0$ limit, the core temperature will change with time according to the law

$$T_{AR}(t) \sim t^{-1}. \qquad (3)$$

The display of the analytical law in Fig. 2 shows that this approximation adequately describes the heat diffusion in the QCL structure. It can be seen that an order of magnitude difference in pulse durations leads to an almost proportional residual superheat, while the largest superheat differs by a factor of about 3.

Under the assumption of fairness of the linear response approximation, when the temperature distribution from previous pulses does not affect the heat transfer dynamics of the current pulse, the core temperature will be determined by the convolution of the core cooling dynamics and the modulated pump signal

$$T_{eq}(t) = \int_{-\infty}^{t} Pump[x]Response[t-x]dx. \qquad (4)$$

A specific feature of the considered problem is that a function of the form t^{-1} is not integrable at infinity, i.e., analytical calculation of the true equilibrium value of the core temperature on an infinite time scale is impossible. However, the specifics of the problem allow a sufficiently accurate quantitative assessment. Taking into account the fact that energy is supplied to the core in portions with a known frequency, let us replace the true equilibrium value of the core temperature by the experimentally observed value, which is formed after some time commensurable with the duration of the experiment:

$$T_{eq} \approx T' f \tau_p \ln(f \tau_{obs}), \qquad (5)$$

where T' — temperature constant proportional to the energy release per pulse, f — pulse delivery frequency, τ_{obs} — duration of the experiment, τ_p — duration of the pump pulse. The logarithmic function is obtained by summing up the contributions from the residual heating, given by the expression (3), due to all pulses applied at the time of observation. The experiment time $t \sim 10^3$ s is taken for the calculations. Using expression (5) for different pulse durations under conditions of unchanged filling factor, in the linear response approximation, it can be obtained that for durations differing by an order of magnitude, the value of the equilibrium temperature will differ by fractions of degrees Kelvin. In particular, for durations of 100 and 1000 ns and a filling factor of 1%, the ratio $\frac{T_{eq}(1000\,\text{ns})}{T_{eq}(100\,\text{ns})} = 0.85$ ($T_{eq}(1000\,\text{ns}) = 1.1\,\text{K}$ and $T_{eq}(100\,\text{ns}) = 1.3\,\text{K}$), i.e., the residual overheating of the active region when pump pulses with a constant filling factor are applied but at different pulse durations (100 and 1000 ns) is actually the same.

The temporal dynamics of heating during pulse delivery in Fig. 2 can be approximated by the following function:

$$T_{imp}(t) = T_a\left(1 - e^{-\frac{t}{\tau_r}}\right) = 20\left(1 - e^{-\frac{t}{300\,\text{ns}}}\right), \qquad (6)$$

where T_a and τ_r — fitting parameters denoting the effective amplitude of the pulse heating temperature and the characteristic time constant of its attainment, respectively. Thus, the average pulse heating, additive (additive) to the steady-state equilibrium value derived in equation (5), will be equal to

$$\langle T_{imp}\rangle(\tau_p) = \frac{1}{\tau_p}\int_0^{\tau p} T_{imp}(t)dt = T_a\left(1 - \frac{\tau_r}{\tau_p}\left(1 - e^{-\frac{\tau_p}{\tau_r}}\right)\right). \qquad (7)$$

Substituting the corresponding values, it can be obtained that $\frac{\langle T_{imp}\rangle(1000\,\text{ns})}{\langle T_{imp}\rangle(100\,\text{ns})} = 4.6$ ($\langle T_{imp}\rangle(1000\,\text{ns}) = 14\,\text{K}$ and $\langle T_{imp}\rangle(100\,\text{ns}) = 3\,\text{K}$). As a result, the average additive heating for long pulses is much greater than that for short pulses. It should be noted again that the equilibrium superheat for both cases is the same.

Thus, the simulation results, taking into account specific parameters, clearly showed that the presence of rapid local overheating of the active region, which is not compensated by the complete cooling of the active region of the QCL during the pause time between pulses, can lead to the intensity drop after pulse durations of 100 ns. The simulation results are well confirmed by the data of Fig. 3, *a*, which shows the experimental dependence of the average power of the QCL output radiation on the filling factor and pulse repetition rate. To obtain this dependence, multiple watt-ampere characteristics were measured for each of the repetition frequencies with increasing pulse duration from a minimum value of 100 ns, which gives the minimum value of the filling factor for each frequency, to the maximum value determined by the observed decrease in the maximum output average optical power. It can be seen from the figure that as the filling factor increases by increasing the repetition rate and decreasing the duration of the pump pulses, the highest average power is achieved. This is due to the fact that when the duration of the pump pulse decreases, less additional heat is generated in the active region of the QCL, which makes it possible to increase the filling factor with an increase in the output average power.

We have experimentally investigated the dependence of the power and threshold characteristics of the QCL on the filling factor when pumping the QCL by current pulses with a duration of 100 ns. Figure 3, *b* shows the dependence of the average power, peak power, and threshold current of QCL on the filling factor. It can be clearly seen that the saturation of the maximum average power occurs at a filling factor of 5%, and the decline occurs after a filling factor of 10%. At the same time, the maximum peak power begins to decrease after a filling factor of 0.3%, and the threshold current does not change significantly until a filling factor of 2.5%. It can be clearly seen from Fig. 3, *c*, where the watt-ampere characteristics of the QCL for various filling factors are given, that no decrease in the differential efficiency is observed up to a filling factor of 2.5% and a pump current amplitude of 3 A, after which the thermal bending of the watt-ampere characteristics becomes the stronger the higher the filling factor. Thus, at an operating voltage of ~ 12 V for a pump current of 3 A, the total power consumption is ~ 36 W, which, with a filling factor of 2.5%, shows that about 1 W of thermal power can be efficiently dissipated from the active region of the QCL without overheating with the chip design used. Further increase of the operating current leads to an increase of the power consumption and, consequently, to QCL overheating. This finding shows that a further increase in the average

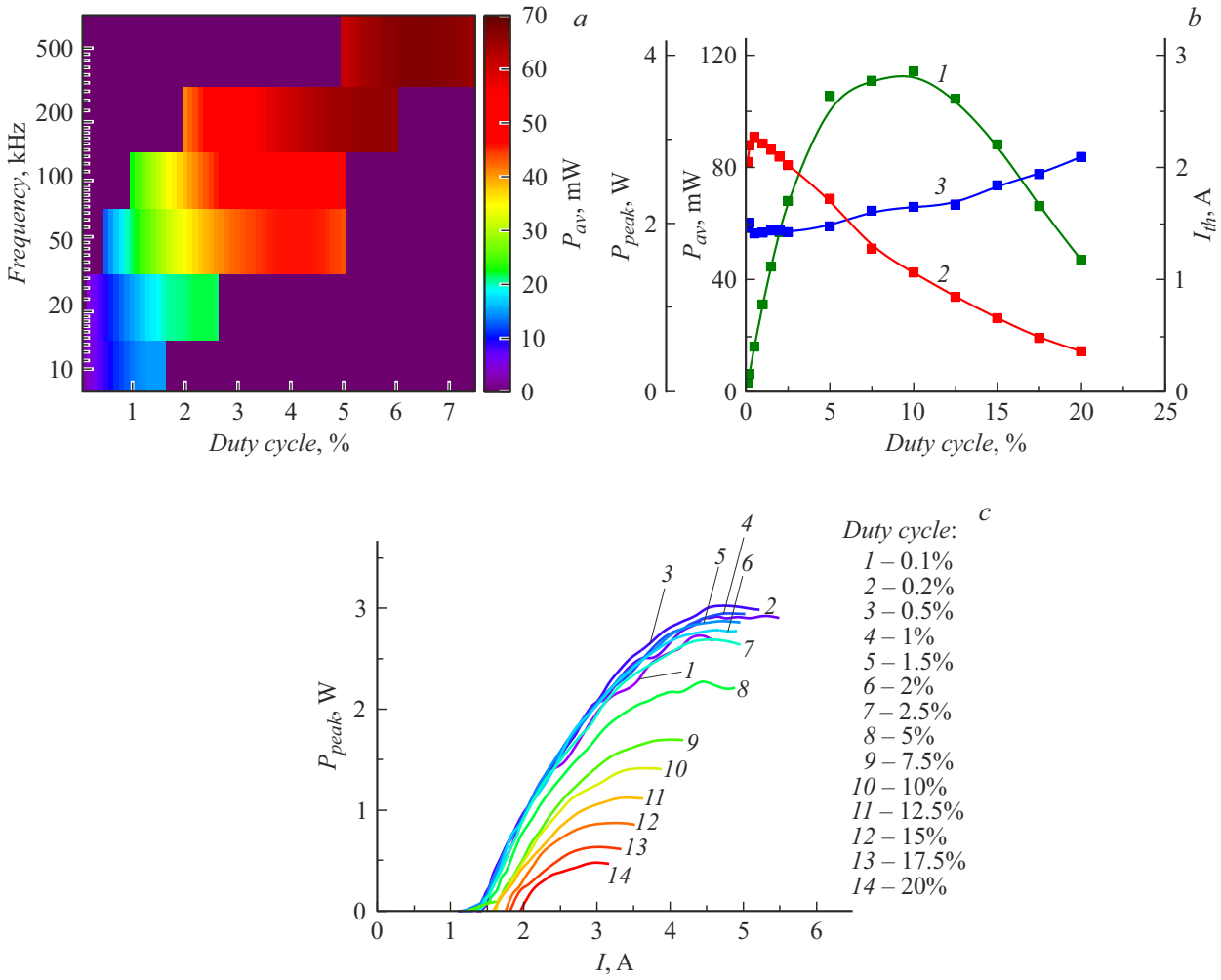

Figure 3. *a* — The dependence of the average output power of the QCL on the filling factor and frequency. *b* — the dependence of average power (*1*), peak power (*2*), and threshold current (*3*) on the filling factor. *c* — watt-ampere characteristics of the QCL for different values of the filling factor. The duration of the current pumping pulse on the *b* and *c* slices was 100 ns. A color version of the figure is provided in the online version of the paper.

power output requires improved approaches to post-growth processing of the structures.

The studies show that to achieve high average power and increase the filling factor while maintaining high peak power, the duration of current pumping pulses should be reduced. In these studies, the minimum duration of current pumping was 100 ns. At the same time, as shown in [12], the on-off delay time of the QCL when pumping with non-zero edge pulses can exceed 5 ns. Therefore, a pump pulse duration range of 20–100 ns appears to be optimal for modulating the QCL with large-amplitude current pulses with a nonzero leading edge. A more precise determination of the pump pulse duration optimum requires additional studies that are beyond the scope of this study.

Thus, the QCL characteristics at different filling factors and different pump pulse repetition rates have been experimentally and theoretically investigated. A maximum average output power of more than 100 mW has been experimentally shown. Further increase of the average power requires providing better heat dissipation from the active region.

Funding of the study

The research was performed under the research program of the National Center for Physics and Mathematics (project „High Energy Density Physics. Stage 2023–2025“).

Conflict of interest

The authors declare that they have no conflict of interest.

References

[1] I.I. Vrubel, E.D. Cherotchenko, D.A. Mikhailov, D.V. Chistyakov, A.V. Abramov, V.V. Dudelev, G.S. Sokolovskii, Nanomaterials, **13** (23), 2994 (2023). DOI: 10.3390/nano13232994

[2] V.V. Dudelev, E.D. Cherotchenko, D.A. Mikhailov, D.V. Chistyakov, S.O. Slipchenko, A.V. Lutetskii, A.G. Gladyshev, A.V. Babichev, L.Ya. Karachinskii, I.I. Novikov, N.A. Pikhtin, A.Yu. Egorov, A.V. Kondrashov, A.A. Semenov, G.S. Sokolovskii, A.B. Ustinov, Tech. Phys. Lett., **49** (11), 71 (2023). DOI: 10.61011/TPL.2025.02.60646.20177.
[3] Y. Deng, Z.F. Fan, B.B. Zhao, X.G. Wang, S. Zhao, J. Wu, F. Grillot, C. Wang, Light Sci. Appl., **11** (1), 7 (2022). DOI: 10.1038/s41377-021-00697-1
[4] M. Joharifar, H. Dely, X. Pang, R. Schatz, D. Gacemi, T. Salgals, A. Udalcovs, Y.-T. Sun, Y. Fan, L. Zhang, E. Rodriguez, S. Spolitis, V. Bobrovs, X. Yu, S. Lourdudoss, S. Popov, A. Vasanelli, O. Ozolins, C. Sirtori, J. Lightwave Techol., **41** (4), 1087 (2023). DOI: 10.1109/JLT.2022.3207010
[5] Y. Bai, N. Bandyopadhyay, S. Tsao, E. Selcuk, S. Slivken, M. Razeghi, Appl. Phys. Lett., **97** (25), 251104 (2010). DOI: 10.1063/1.3529449
[6] F. Wang, S. Slivken, D.H. Wu, M. Razeghi, AIP Adv., **10** (7), 075012 (2020). DOI: 10.1063/5.0012925
[7] F. Wang, S. Slivken, D.H. Wu, M. Razeghi, Opt. Express, **28** (12), 17532 (2020). DOI: 10.1364/OE.394916
[8] W. Zhou, Q.-Y. Lu, D.-H. Wu, S. Slivken, M. Razeghi, Opt. Express, **27** (11), 15776 (2019). DOI: 10.1364/OE.27.015776
[9] V.V. Dudelev, E.D. Cherotchenko, I.I. Vrubel, D.A. Mikhailov, D.V. Chistyakov, V.Yu. Mylnikov, S.N. Losev, E.A. Kognovitskaya, A.V. Babichev, A.V. Lutetskiy, S.O. Slipchenko, N.A. Pikhtin, A.V. Abramov, A.G. Gladyshev, K.A. Podgaetskiy, A.Yu. Andreev, I.V. Yarotskaya, M.A. Ladugin, A.A. Marmalyuk, I.I. Novikov, V.I. Kuchinskii, L.Ya. Karachinsky, A.Yu. Egorov, G.S. Sokolovskii, Phys. Usp., **67** (1), 92 (2024). DOI: 10.3367/UFNe.2023.05.039543.
[10] E. Cherotchenko, V. Dudelev, D. Mikhailov, G. Savchenko, D. Chistyakov, S. Losev, A. Babichev, A. Gladyshev, I. Novikov, A. Lutetskiy, D. Veselov, S. Slipchenko, D. Denisov, A. Andreev, I. Yarotskaya, K. Podgaetskiy, M. Ladugin, A. Marmalyuk, N. Pikhtin, L. Karachinsky, V. Kuchinskii, A. Egorov, G. Sokolovskii, Nanomaterials, **12** (22), 3971 (2022). DOI: 10.3390/nano12223971
[11] V.V. Dudelev, D.A. Mikhailov, A.V. Babichev, G.M. Savchenko, S.N. Losev, E.A. Kognovitskaya, A.V. Lyutetskii, S.O. Slipchenko, N.A. Pikhtin, A.G. Gladyshev, D.V. Denisov, I.I. Novikov, L.Ya. Karachinsky, V.I. Kuchinskii, A.Yu. Egorov, G.S. Sokolovskii, Quantum Electron., **50** (11), 989 (2020). DOI: 10.1070/QEL17396
[12] E.D. Cherotchenko, V.V. Dudelev, D.A. Mikhailov, S.N. Losev, A.V. Babichev, A.G. Gladyshev, I.I. Novikov, A.V. Lutetskiy, D.A. Veselov, S.O. Slipchenko, N.A. Pikhtin, L.Ya. Karachinsky, D.V. Denisov, V.I. Kuchinskii, E.A. Kognovitskaya, A.Yu. Egorov, R. Teissier, A.N. Baranov, J. Lightwave Technol., **40** (7), 2104 (2022). DOI: 10.1109/JLT.2021.3134837

Translated by J.Savelyeva